Weather and Climate Extremes 17 (2017) 36–46

Contents lists available at ScienceDirect

Weather and Climate Extremes

journal homepage: www.elsevier.com/locate/wace

Detecting the effect of urban land use on extreme precipitation in the Netherlands

Vahid Rahimpour Golroudbary*, Yijian Zeng, Chris M. Mannaerts, Zhongbo (Bob) Su

Faculty of Geo-Information Science and Earth Observation (ITC), Department of Water Resources, University of Twente, Enschede, The Netherlands

ARTICLE INFO

Keywords:
Precipitation extremes
Indices
Spatial pattern
Trend analysis
FTPW
Urban land use
The Netherlands

ABSTRACT

A notable increase in heavy precipitation has been observed over the Netherlands in recent decades. The aim of this study was to assess the influences of urban land use on these extreme precipitation patterns. Significant differences between an earlier multi-decadal period and a recent period were found in the Netherlands between 1961 and 2014. The significant changes in different indices indicate that severe precipitation events were not distributed homogeneously across the study area. The precipitation probability and distribution were assessed using the block maxima approach by comparing observations from urban and rural areas at different timescales. The possible effects of land use on extreme precipitation were assessed by quantifying the differences between urban and rural rain gauge stations according to the spatial gridding method. This study shows that urban land use may have affected the extreme precipitation patterns across the Netherlands. The data from all the categorized stations show that urban areas receive more intense extreme precipitation than do rural areas. Relative to other areas in the Netherlands, the urban areas in the western populated regions of the country exhibit prominent urban land use influences on the extreme precipitation patterns.

1. Introduction

Human life is more directly affected by precipitation than any other atmospheric phenomenon (Levizzani et al., 2002); thus, detecting changes in precipitation has become a critical research focus in recent decades (Hanel and Buishand, 2010). Extensive work has been dedicated to studying extreme precipitation events (Aguilar et al., 2009; Chen et al., 2012; Griffiths et al., 2005; Gutowski et al., 2010; Trenberth et al., 2007; van den Besselaar et al., 2012; Wang and Zhang, 2008; Westra et al., 2013; Willems, 2013a,b). Studies above have shown that precipitation and extreme events have increased at higher latitudes and that the intensity and frequency of extreme precipitation events have intensified. Physically, changes in the North Atlantic Oscillation (NAO) and the sea surface temperature (SST) are the major sources of precipitation changes in the Northern Hemisphere (Hurrell, 1995; Jones et al., 1997; Lenderink et al., 2009). In addition, several studies have shown that land use and topography can affect regional climates. Thus, extreme precipitation patterns can be influenced by the type of land use in high-latitude regions.

The Netherlands is located along the North Sea. Recent studies have revealed that the total precipitation and frequency of extreme events have increased over a large part of the Netherlands (Burauskaite-Harju et al., 2012; van Haren et al., 2013; Daniels et al., 2014; Rahimpour Golroudbary et al., 2016). Buishand et al. (2013) concluded that precipitation over the Netherlands increased by approximately 26% during the period from 1910 to 2013. Furthermore, Ter Maat et al. (2013) investigated the combined effects of forestation and topography on the maximum rainfall in the Netherlands and found that elevated forest areas (with a maximum elevation of 100 m) in the middle of the country received more precipitation than did the surrounding areas. Hurk et al. (2014) reported that the intensity of extreme precipitation in the western regions (including the most urbanised areas) was greater than that in the other regions of the Netherlands. The various physical and chemical processes (such as the Bowen ratio, heat storage capacity, and surface roughness) could be responsible for the effects of urban areas on precipitation (Oke, 1982; Shepherd, 2006; Mitra et al., 2012). Further studies also concluded that urbanisation effects on precipitation should be considered in the Netherlands (Daniels et al., 2015a,b).

This study investigates the variability in extreme daily precipitation and its spatial patterns across the Netherlands. The main objective is to

* Corresponding author. Faculty of Geo-Information Science and Earth Observation (ITC), Department of Water Resources, University of Twente, P.O. Box 352, 7500 AE, Enschede, The Netherlands.

E-mail addresses: V.rahimpourgolroudbary@utwente.nl, Rahimpour.vahid@gmail.com (V. Rahimpour Golroudbary).

http://dx.doi.org/10.1016/j.wace.2017.07.003
Received 20 September 2016; Received in revised form 29 June 2017; Accepted 24 July 2017
Available online 9 August 2017
2212-0947/© 2017 The Authors. Published by Elsevier B.V. This is an open access article under the CC BY-NC-ND license (http://creativecommons.org/licenses/by-nc-nd/4.0/).

analyse variations in extreme precipitation in three climatological periods and identify the likely discrepancy in extreme precipitation between urban and nonurban (rural) areas in the Netherlands. The link between the land use types and the monthly daily precipitation maxima was found by categorising stations in the Netherlands as urban or rural according to their local environmental characteristics (land use and surface features). This method is based on high-quality, historically observed precipitation data and the calculation of extreme precipitation indices and individual time series of the monthly daily precipitation maximum across the country.

In the following section, the precipitation data, precipitation indices, methods used in statistical analysis, and urban and rural stations are introduced. In section 3, the results and analysis of the trends in the observed indices are presented; the monthly amounts and trends during the different climatological periods are compared, and the regional differences in extreme precipitation are investigated. In section 4, the discussion is presented, and the conclusions are in section 5.

2. Materials and methods

2.1. Precipitation data

Long-term precipitation data from manual rain gauges in the Netherlands were quality controlled and validated (Buishand et al., 2013). These rain gauges reported daily precipitation (more details are provided at http://www.knmi.nl). The homogenised dataset was statistically tested and described by Buishand et al. (2013), and only a negligible difference in the detection of trends in extreme indices was observed between the homogenised dataset and the original quality-controlled dataset. A total of 231 rain gauges were used in this study, and the record length was 54 years (1961–2014). Complete data were available for 80% of the gauges, and missing data represented less than 1% of the data from the remaining gauges for this period. The missing data were replaced by values from ECAD (European Climate Assessment & Dataset) datasets (Klein Tank et al., 2002). The rain gauges have reasonable spatial coverage (with a spacing of approximately 10 km), and ordinary kriging was used to grid the precipitation data at a 1 km resolution (for a more detailed discussion, see Sluiter (2009, 2012, 2014)).

2.2. Definition of the precipitation indices

Extreme precipitation indices were defined to provide a true perspective of the observed changes based on the characteristics of the extreme events, including their frequency, amplitude, and persistence (Klein Tank et al., 2009). Extreme precipitation indices have been comprehensively described and classified into two groups (Zhang and Yang, 2004; Zhang et al., 2005; De Lima et al., 2010; Tian et al., 2011; Maragatham, 2012). The first group defines absolute thresholds and enumerates the number of days exceeding a certain absolute precipitation value, whereas the second group is based on percentile thresholds. The number of days exceeding a certain percentile threshold (representing the frequency of threshold crossing) is fixed for the World Meteorological Organization (WMO) base period (1961–1990). The specific indices used for this study are shown in Table 1. The details of the index definitions and calculations are described in Klein Tank et al. (2009). The extreme precipitation indices were calculated by using RClimDex (Zhang and Yang, 2004) software package in the R environment (R Foundation for Statistical Computing, Vienna, 2011).

2.3. Statistical analysis

This study investigated long-term time series data (period I: from year 1961–2014):

$$X_k = x_i,\ \ x_{i+1},\ \ \ldots,\ \ x_p \tag{1}$$

Table 1
Definition of the extreme indices for precipitation (P).

Indices	Indicator description (units)
Px1	Monthly maximum 1-day precipitation (mm)
Px5	Monthly maximum consecutive 5-day precipitation (mm)
Ptot	Annual total precipitation in wet days P ≥ 1 mm (mm)
SDII	Average daily precipitation amount on wet days (mm/day)
P10 mm	Annual count of days when P ≥ 10 mm (days)
P20 mm	Annual count of days when P ≥ 20 mm (days)
P30 mm	Annual count of days when P ≥ 30 mm (days)
CWD	Maximum number of consecutive wet days with P ≥ 1 mm (days)
P95Ptot	Annual total P (between 1961 and 2014) when P > 95th percentile of precipitation for the 1961–1990 period (%)
P99Ptot	Annual total P (between 1961 and 2014) when P > 99th percentile of precipitation for the 1961–1990 period (%)

where i = 1961, p = 2014, and k = 1, 2, …, 231. The time series of extreme values for each station (X_k) was divided into two multi-decadal periods as follows:

$$X_{k\_A} = x_i,\ \ x_{i+1},\ \ \ldots x_m \qquad \text{and} \qquad X_{k\_B} = x_{m+1},\ \ x_{m+2},\ \ \ldots x_p \tag{2}$$

where $m = \left(\frac{p+i}{2}\right)$, and the two multi-decadal periods in this study are defined as period II (from 1961 to 1987) and period III (from 1988 to 2014). The calculated value for *m* is rounded down to the nearest integer (i.e., 1987.5 rounded down to 1987).

The time series anomalies (D_{ki}) are calculated by considering the climatological average ($\overline{X}_k$) relative to the WMO base period (1961–1990) ($\overline{X}_{k\_WMO}$) for each station (k) as follows:

$$\overline{X}_k = \frac{\sum_{i=1961}^{2014}(x_i)}{54},\ \ \overline{X}_{k\_WMO} = \frac{\sum_{i=1961}^{1990}(x_i)}{30} \tag{3}$$

$$D_{ki} = \left(\frac{x_i - \overline{X}_{k\_WMO}}{\overline{X}_k}\right) * 100 \tag{4}$$

where x_i is defined as in Equation (1) and PD_{ki} is the percentage anomaly for each station (k) and year (1961 ≤ *i* ≤ 2014). The overall percentage anomaly (PD_i) over the country (i.e. 231 stations) for each year *i* is defined as follows:

$$PD_i = \frac{\sum_{k=1}^{231} D_{ki}}{231} \tag{5}$$

The variation in precipitation could be observed visually or investigated using statistical methods (i.e., the hypothesis test). A broad range of parametric and non-parametric methods have been used to investigate trends in extreme precipitation in previous studies (Arnbjerg-Nielsen et al., 2013). In this study, the variations in precipitation observations were investigated using the Mann-Kendall test (Kendall, 1948; Mann, 1945) because of the non-Gaussian distributions of the observations.

In the Mann–Kendall test, the null and alternate hypotheses (H_0 and H_1) of the trend test are that no trend exists and that a monotonic trend exists in the time series, respectively. The Mann-Kendall statistical test is expressed as follows:

$$S = \sum_{i=1961}^{p-1} \sum_{j=i+1}^{p} sgn\ (X_j - X_i) \tag{6}$$

where X_j and X_i are sequential data. The term $sgn\ (X_j - X_i)$ is defined as follows:

$$sgn\left(X_j - X_i\right) = \begin{cases} +1 & if \quad \left(X_j - X_i\right) > 0 \\ 0 & if \quad \left(X_j - X_i\right) = 0 \\ -1 & if \quad \left(X_j - X_i\right) < 0 \end{cases} \tag{7}$$

When $n \geq 8$, the mean of S (E(s) = 0) and variance is normally distributed:

$$VAR(S) = \frac{1}{18}\left[n(n-1)(2n+5) - \sum_{q=1}^{n} t_q\left(t_q - 1\right)\left(2t_q + 5\right)\right] \tag{8}$$

where n is the length of the time series and t_q is the number of occurrences of the qth value, (q = 1, 2, …, 54). The normalized statistic test Z_S can be expressed as follows:

$$Z_S = \begin{cases} \frac{S-1}{\sqrt{VAR(S)}} & if \quad S > 0 \\ 0 & if \quad S = 0 \\ \frac{S+1}{\sqrt{VAR(S)}} & if \quad S < 0 \end{cases} \tag{9}$$

In a two-tailed test, when $|Z_S| > Z_{1-\alpha/2}$, the H0 hypothesis (no trend) can be rejected because the $|Z_S|$ value is larger than the critical value at the chosen significance level of the test (for this study α = 0.05 and $Z_{1-\alpha/2} = \pm 1.96$.).

The strength of the trend was calculated based on the Theil–Sen's slope (Theil, 1950; Sen, 1968), which is known as a nonparametric linear regression slope (β). This method calculates the overall slope using the median of the slopes of all the pairs of sequential data (X_j and X_i). The nonparametric estimate is expressed as following:

$$\beta = \text{Median}\left[\frac{X_j - X_i}{j - i}\right] \quad \text{for all} \quad j > i \tag{10}$$

The autocorrelation in time series can affect the result of the Mann–Kendall test (von Storch, 1995). The Yue et al. (2002) approach (FTPW) proposed a modified pre-whitening for the Mann–Kendall trend to reduce effectively the impact of autocorrelation. In the FTPW approach, if the slope (estimated with the Theil–Sen's slope) differs from 0, the data are detrended by the slope as follows:

$$X_{detrend\_n} = X_{original\_n} - \beta.n \tag{11}$$

where $X_{original\_n}$ and $X_{detrend\_n}$ are the original and detrended time series at time n, respectively. Subsequently, the noise from the detrended time series is removed by a lag 1 autoregressive (AR (1)) coefficient:

$$X'_{detrend\_n} = X_{detrend\_n} - r_1 . X_{detrend\_n-1} \tag{12}$$

where $X'_{detrend\_n}$ is the residual and r_1 is the autocorrelation coefficient. The trend is then added back to the time series values. The $X''_{detrend\_n}$ demonstrates the linear trend without the autocorrelation noise.

$$X''_{detrend\_n} = X'_{detrend\_n} + \beta.n \tag{13}$$

Finally, the Mann-Kendall test is applied to the adjusted time series to measure the significance of the trend (Yue et al., 2003).

The magnitude of daily precipitation varies from one station to another. Therefore, the temporal variability of spatial averages of Px1 may be dominated by the stations with large Px1 variations. To reduce this effect we used the standardized data for Px1 at each station by transforming the data to the probability-based index (PI). To detect the monthly maximum daily precipitation (Px1) differences between urban and rural areas, the observed values are normalized to the PI index between zero to one by the fitting of a generalized extreme value (GEV) (Min et al., 2009). The study assumes that the Px1 for an individual month follows the GEV distribution function as follows:

$$PI = F(P_i;\ \mu,\ \sigma,\ \mathcal{E}) \tag{14}$$

$$F(x;\ \mu,\ \sigma,\ \mathcal{E}) = \begin{cases} exp\left(-\left[1 + \mathcal{E}\frac{x-\mu}{\sigma}\right]^{-\frac{1}{\mathcal{E}}}\right), & \mathcal{E} \neq 0 \\ exp\left(-exp\left(-\frac{x-\mu}{\sigma}\right)\right), & \mathcal{E} = 0 \end{cases} \quad \begin{cases} \mu \in R \\ \sigma > 0 \\ \mathcal{E} \in R \end{cases} \tag{15}$$

where the monthly maximum precipitation in year i (P_i) is defined by location (μ), scale (σ) and shape parameters ($\mathcal{E}$). The GEV parameters were estimated via the maximum likelihood estimation (Jenkinson, 1955) and bootstrap method (10^4 replicate sample sizes).

2.4. Classification of station types

A clear, unified definition is not available for determining the land use extents. Specifically, for mapping the urban extent, different approaches are available based on population density, satellite images and other maps (Schneider et al., 2009). Different datasets can lead to different boundaries between urban and rural areas, resulting in different station classifications. Therefore, we used the Co-ORdination of INFormation on the Environment (CORINE) database, which was used in the previous studies of Chrysanthou et al. (2014) and Daniels et al. (2014) to distinguish between urban and rural areas in the Netherlands. In this study, the CORINE land cover at 100*100-m resolution for the year 2012 (EEA, 2014) was applied to classify the stations into urban and rural subsets. The urban extent was defined by six land cover categories, i.e., i) discontinuous urban fabric; ii) industrial or commercial units and public facilities; iii) road and rail networks and associated land; iv) port areas and airports; v) mineral extraction sites, dump sites, and construction sites; and vi) green urban areas and sport and leisure facilities. Suomi et al. (2012) concluded the footprint of the urban heat island (UHI) effect is approximately 5 km. Therefore, the area within a 5 km radius of the rain gauge stations was extracted to identify the land cover types. The stations where the six urban land cover categories represented more than a quarter of the surrounding area were classified as urban stations, and the others were defined as rural stations (Daniels et al., 2014). The urban and rural station subsets were created via spatial gridding, which is also employed in climate monitoring by NOAA/NCDC (Hausfather et al., 2013).

Daniels et al. (2014) found that the distance from the coast had a greater effect on precipitation changes than did other surface characteristics in the Netherlands. They concluded that the SST influence on extreme summer precipitation in the Netherlands is confined to within 25 km of the coast. Lenderink et al. (2009) showed that SSTs have a strong influence on regions within 50 km of the coast. To account for the effect of distance from the coast on precipitation, four regions were classified to investigate the differences among the subsets of urban and rural stations. The stations were considered in four regions: A, B, C, and D, which are located 0–25 km, 25–50 km, 50–100 km, and 100–200 km from the coast, respectively (Daniels et al., 2014). Each defined region contained a sizeable fraction (between 20% and 30%) of the total stations in the Netherlands. Accordingly, the four regions were used to classify the individual urban and rural station subsets for each region (Table 2). Fig. 1 shows the distributions of urban and rural stations with respect to the defined regions.

As shown in Table 2, the mean elevations of the rain gauges in the defined urban and rural subsets are similar. Therefore, similar topographic effects on precipitation are expected for the urban and rural subsets in a given region. The population of each subset was averaged based on the extracted population within 5 km of each station on 1 January 2015 (available at the Dutch national statistical institution website) (CBS, 2015). The average population in the vicinity of the urban

Table 2
Number of stations in the urban and rural subsets in different regions. The annual maxima of daily precipitation (mm) averaged for the urban and rural stations in each region during the 54-year period (I) and two multi-decadal periods (II and III) are also listed.

Region	Dominant soil types	subset	Number of stations	I (mm)	II (mm)	III (mm)	Mean Population	Mean Elevation (m)
A	Clay and peat	Urban	15	36.3	34.2	38.5	127710	0
		Rural	46	35.3	32.8	37.8	17059	1
B	Clay	Urban	5	35.6	34.4	36.1	102672	0
		Rural	46	34.5	32.6	36.3	39349	1
C	Sand and loam	Urban	10	35	32.8	37.4	57900	10
		Rural	62	34.7	33.1	36.2	27342	9
D	Sand	Urban	12	33.3	32.2	34.4	75205	38
		Rural	35	34.4	32.9	35.8	22797	35
Countrywide		Urban	42	35	33.3	36.7	93106	13
		Rural	189	34.7	32.9	36.5	26920	10

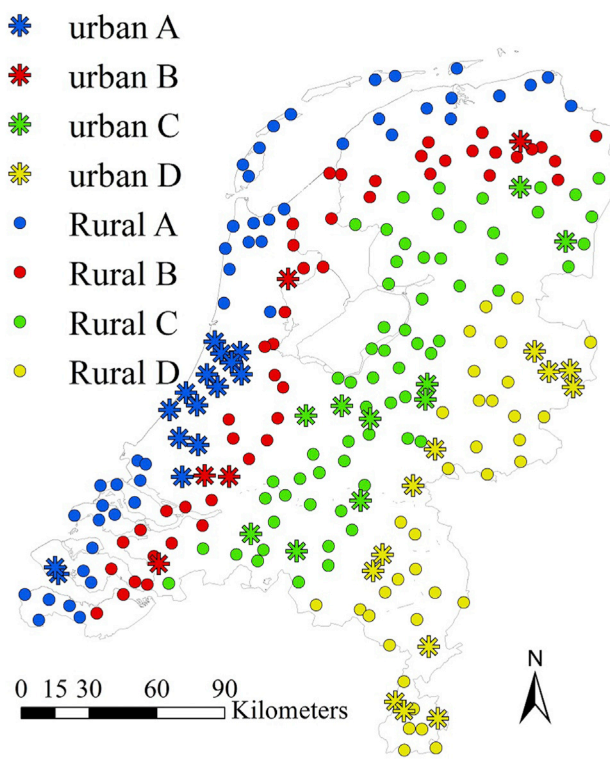

Fig. 1. Distribution of urban (asterisk) and rural (circles) stations in the Netherlands. The regions A, B, C and D are represented by symbols coloured blue, red, green, and yellow, respectively.

stations in region A is greater than those of the other regions. Moreover, the largest difference in the average population between the urban and rural stations exists in regions A and B in the western Netherlands.

3. Results

In this section, the results of the analysis of the extreme precipitation indices across the Netherlands are presented, and the 1-day maximum precipitation values (Px1) in different individual months are investigated. The influence of urban land use on extreme precipitation is assessed based on the results for extreme indices and the categorized stations across the country. The regional features of urban land use effects on extreme precipitation were assessed via the analysis of urban-impacted Px1 in the four defined regions (section 3.3).

3.1. Changes in extreme precipitation indices

The results in Fig. 2 show that almost all of the indices have increased throughout the Netherlands during the last 54 years and the recent multi-decadal period (except for CWD). The changes in the indices in period II (i.e. from 1961 to 1987) were smaller than those in period III (i.e. from 1988 to 2014), indicating that most of the index changes occurred during the recent multi-decadal period.

Fig. 2 presents the spatial pattern of the index changes between the two multi-decadal averages (e.g. Period III – Period II) over the Netherlands. Fig. 2(a) and (b) show the changes in the monthly maxima of 1-day and 5-day precipitation (Px1 and Px5), respectively, thereby illustrating the variations in extreme precipitation. The Px1 changes are positive in the recent multi-decadal period (period III) throughout the Netherlands except in the southeast of the country. The Px5 changes are positive for most stations, especially in the east of the country.

Buishand et al. (2013) claimed that the mean annual rainfall amount on the western side of the Netherlands increased over the last century. The overall increase in the Ptot data (Fig. 2(c)) confirms this result, and positive changes have been observed, especially for stations in the western part of the country. Moreover, in Fig. 2(d), the simple precipitation intensity index (SDII) shows positive changes for a large part of the country in the recent multi-decadal period. The long tail of the frequency distribution of extreme precipitation may be strongly affected by a slight increase in the average (Groisman et al., 1999). Therefore, the positive changes in the total annual precipitation are associated with an upward slope for changes in heavy precipitation events (such as the P10 mm, P20 mm and P30 mm indices). The changes in heavy precipitation events between the two multi-decadal averages are mostly positive throughout the country (Fig. 2(e–g)).

Significant changes are not observed in the consecutive wet day indices (i.e., CWD) across the Netherlands (Fig. 2(h)). The CWD shows positive changes clearly larger in the western and southwestern regions than the rest of the country. P95Ptot and P99Ptot represent the 95th and 99th percentiles of wet days, respectively. Fig. 2(i) and (j) demonstrate the changes between two multi-decadal averages in percentile exceedance for the very wet days (P95Ptot) and extremely wet days (P99Ptot). These indices show that the increasing change in extreme precipitation is more rapid and disproportionate compared with that of the annual total precipitation across the Netherlands.

In addition to the estimated changes in the indices between the averages of the two multi-decadal periods, the data were assessed to identify long-term changes in recent years in the Netherlands. The index time series were averaged spatially over all stations in order to calculate the differences between each year of the index time series and the WMO base period (1961–1990). Fig. 3 shows the result of this analysis for each index. Most of the plots related to extreme precipitation show positive, statistically significant annual changes. The observed changes in the wet indices (P10 mm, P20 mm, P30 mm, P95Ptot and P95Ptot) represent significant positive trends, resulting in larger annual values.

3.2. Assessing the monthly maxima of daily precipitation

The maximum daily precipitation (Px1) index is the most widely used extreme precipitation index for hydrological applications. The analysis of

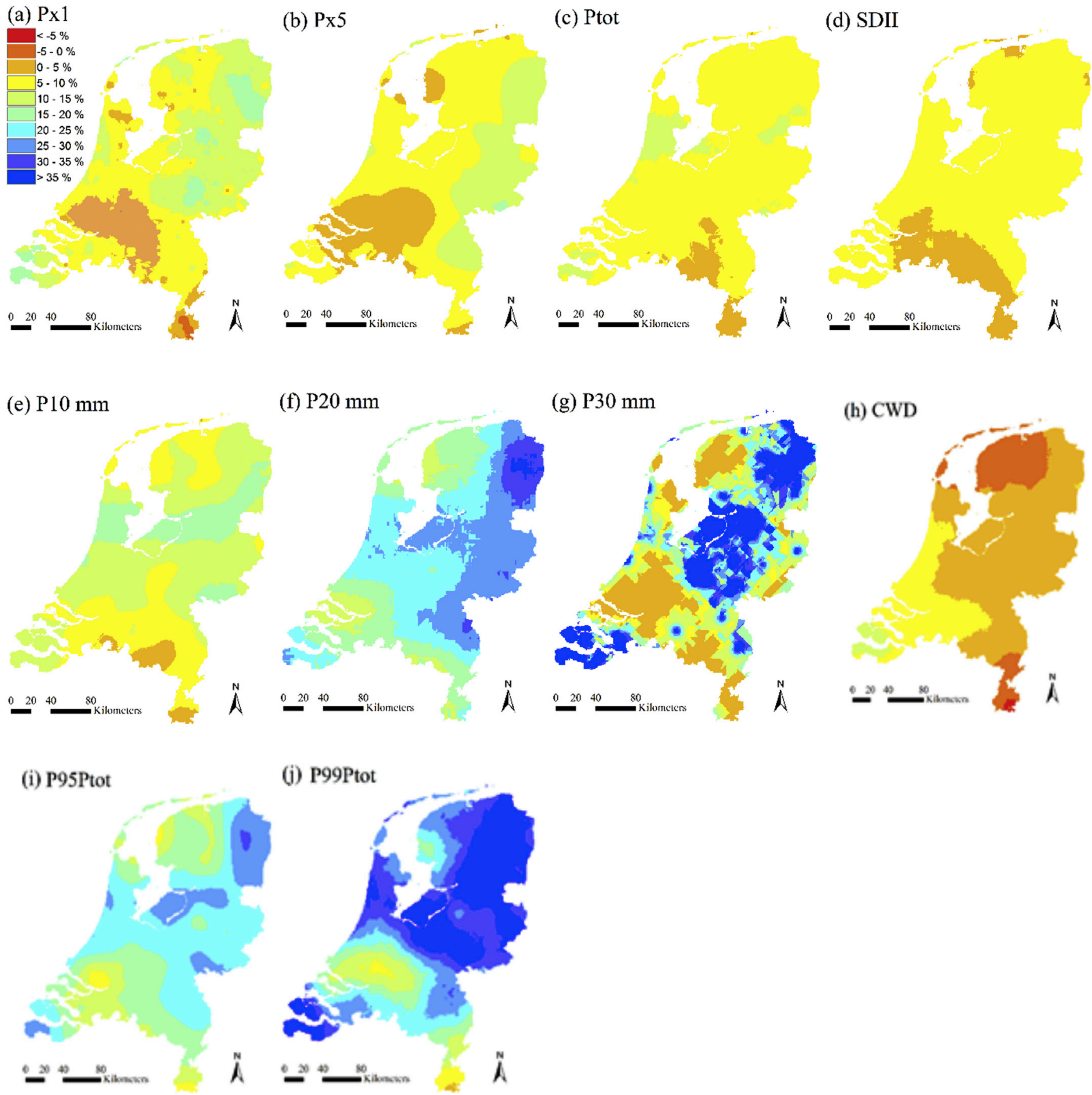

Fig. 2. Spatial distributions of extreme precipitation changes (%) during two multi-decadal periods from 1961 to 2014. The ordinary Kriging interpolated changes for the indices are shown. The maps from top to bottom, right to left (a–j) represent Px1, Px5, Ptot, SDII, P10 mm, P20 mm, P30 mm, CWD, P95Ptot, and P99Ptot, respectively.

Px1 could provide a better understanding of the impacts of extreme precipitation on human life, infrastructure, agriculture, and socioeconomic systems (Nicholls and Alexander, 2007; Min et al., 2011). In the following, the Px1 index, which was considered to be representative of the extreme precipitation indices, was used to assess the extreme precipitation variations for individual months (from January to December).

The rain gauge data were separated into monthly blocks of data, and the maximum daily precipitation values and the associated trend were determined for each block. The Px1 amount for the periods III and II and the trends are shown in Fig. 4. It shows that the monthly Px1 amounts are greater in period III than in period II. The presented differences between periods III and II based on Px1 (hereafter as $\Delta_{III\text{-}II}$Px1) indicate that the largest monthly $\Delta_{III\text{-}II}$Px1 amounts occur in July and August. Moreover, the smallest (negative) $\Delta_{III\text{-}II}$Px1 amounts occur in June. For the trend, the smallest difference (negative) occurs in March, and the largest $\Delta_{III\text{-}II}$Px1 trends occur in July and August. The $\Delta_{III\text{-}II}$Px1 trends have increased more in the summer half-year (May–October) than in the winter half-year (November–April).

3.3. Impact of urban land uses on extreme precipitation

This section investigates the extreme indices for the urban areas in the

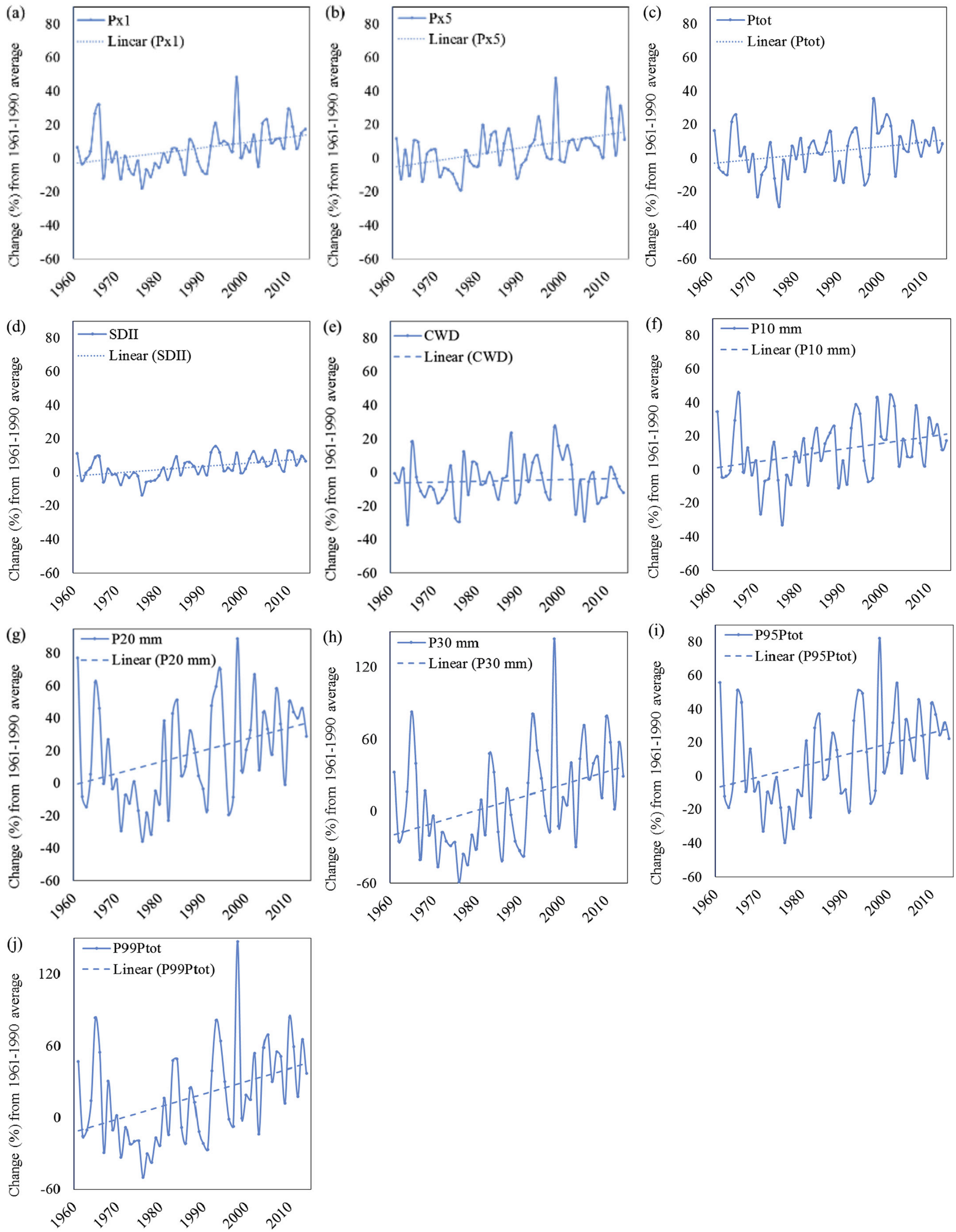

Fig. 3. The panels from (a) to (j) show the analysis of time series of extreme indices during two multi-decadal periods over the last 54 years for Px1, Px5, Ptot, SDII, CWD, P10 mm, P20 mm, P30 mm, P95Ptot, and P99Ptot respectively. The solid and dotted lines show the indices and the least square fit weighted by linear regression analysis for 1961–2014. The difference between the average of each extreme index from 1961 to 2014 and the average from 1961 to 1990 supports the pattern of index changes shown in Fig. 2.

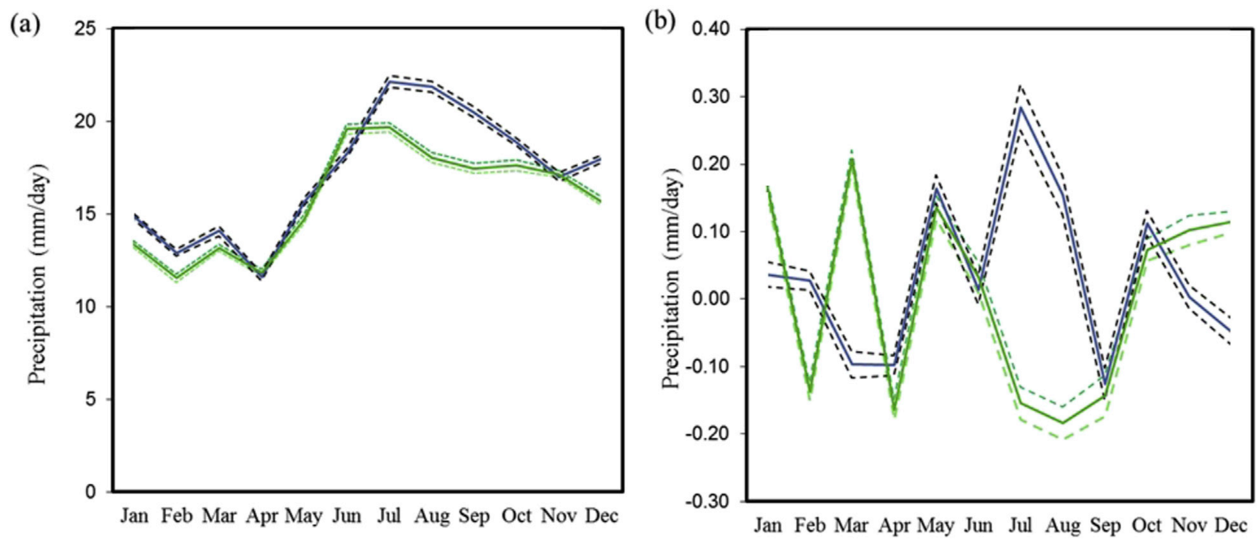

Fig. 4. Px1 monthly variation for amount (a) and trend (b) during the period II (green line) and period III (blue line) in 95% confidence intervals (dashed lines).

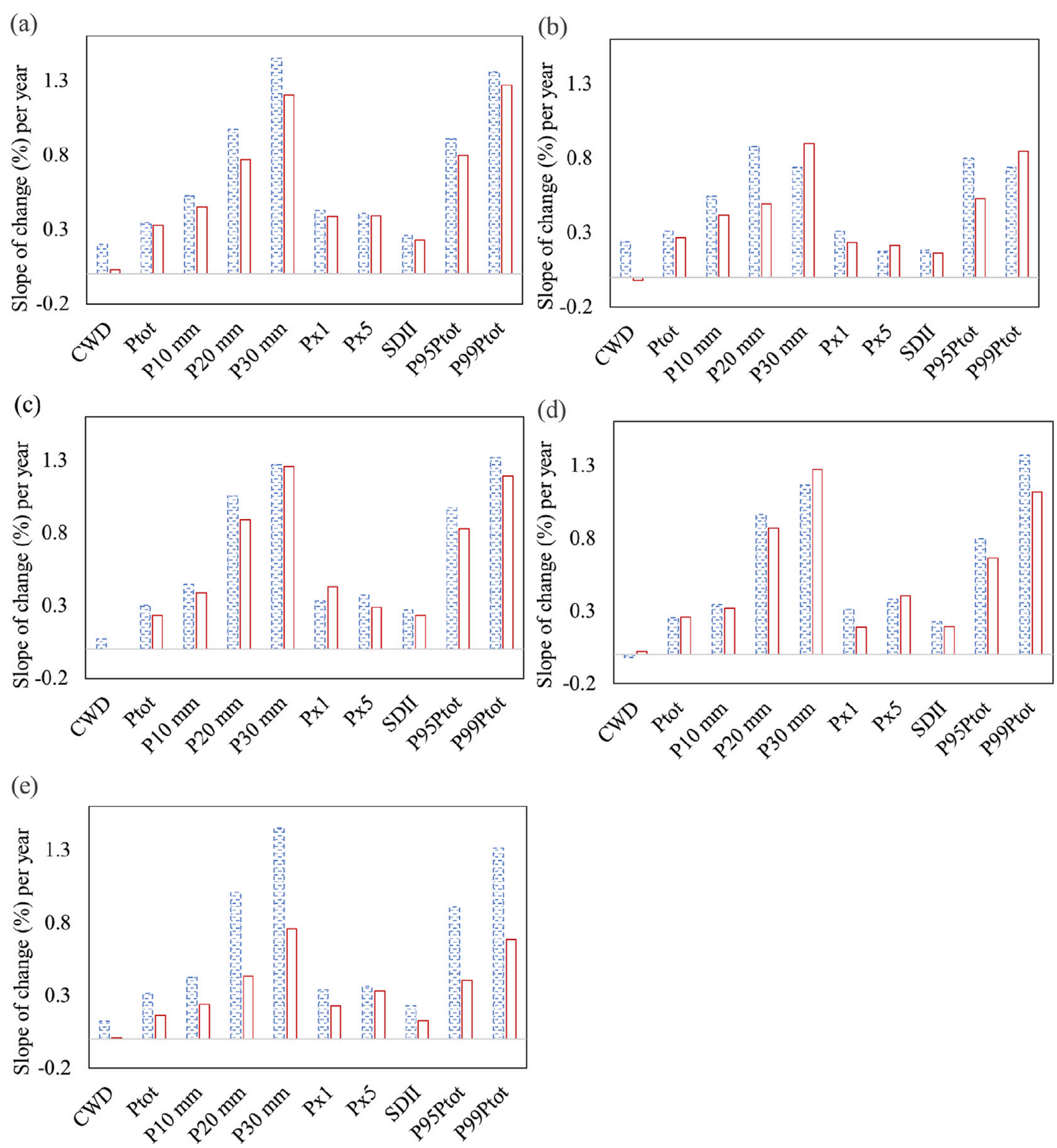

Fig. 5. The slope of extreme precipitation index changes from the 1961–1990 average across the regions A to D (from (a) to (d)) and whole country (e) for urban (blue dashed columns) and rural (red columns) stations. The slopes were calculated using the Theil–Sen's slope, and the statistical significance was estimated by the Mann-Kendall test. The estimated changes are statistically significant at $\alpha = 0.05$ for all indices with some exception (CWD for all regions, P20 mm for rural in region B, Px1 for rural in region B and D, Px5 in urban region B).

Netherlands with respect to the defined regions (i.e., regions A, B, C and D). This investigation is then followed by a detailed analysis of the effects of urban land use on the Px1 index on a monthly basis. Then, the regional features of the differences in the Px1 index between the urban and rural areas are investigated.

3.3.1. Overall features of urban-impacted extreme indices

The slopes of indices changes relative to the 1960–1990 average were estimated for the urban and rural stations between 1961 and 2014 throughout the Netherlands (Fig. 5). The stations across the country were divided into two groups, urban stations and rural stations (see section 2.3). The investigated indices exhibited positive trends with respect to the 1961–1990 average at the urban and rural stations during period I. The pattern of index changes for the urban stations was similar to that for the rural stations. The positive changes in the extreme indices of the urban stations are relatively higher than those of the rural stations throughout 54-year period. In Fig. 5, the overall slopes of the index changes with respect to the 1961–1990 average were steeper for the urban stations than for the rural stations during the recent multi-decadal period.

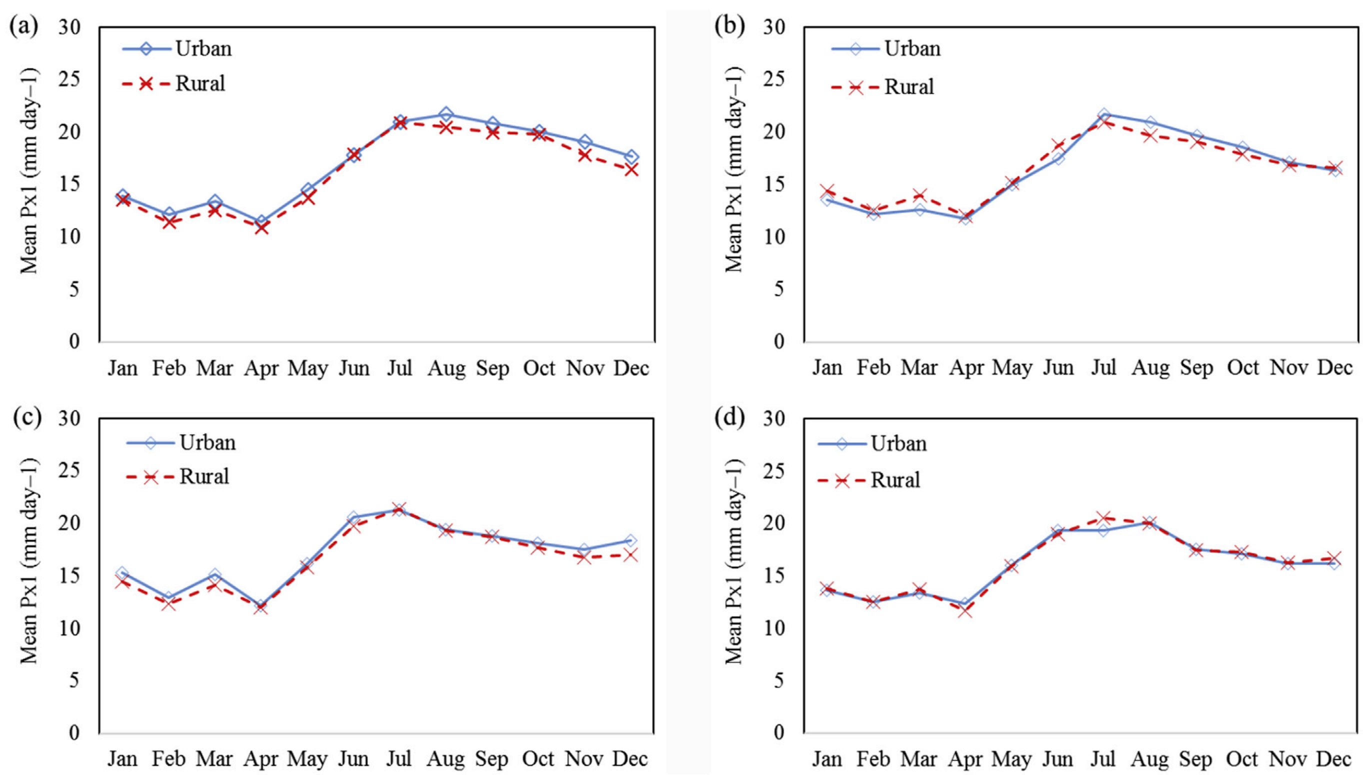

Fig. 6. Panels (a–d) show the mean of Px1 amounts (mm) for the urban stations (blue line) and rural stations (dashed line) across the regions (A, B, C, and D) between 1961 and 2014.

3.3.2. Monthly features of urban-impacted Px1

The results in Fig. 6 show that the regions A and B show similar patterns of Px1 variations and exhibit relatively high values in August. In contrast, the Px1 values are higher in June and July in the regions C and D. The Px1 mean for region A is slightly higher in the urban areas than in the rural areas between 1961 and 2014. These differences in Fig. 6 are easier to distinguish for regions A and B due to the greater variation rather than the rest regions. Between August and November, the Px1 values are higher in the urban areas in region A than in other regions. The Px1 values are also higher in the urban areas than in the rural areas in region B between July and November. The urban Px1 is higher than the rural one in region C for all months but July, and in region D for 7 months other than January, March, May, July, and December.

The Px1 index trends were further analysed across the urban and rural areas in the Netherlands for the individual months. Owing to the uncertain estimated means of the monthly Px1 time series and the inhomogeneity in the Px1 time series for the urban and rural areas, the values of the monthly Px1 index from each station are standardized before estimating the urban and rural averages (Min et al., 2011). The standardized monthly maximum precipitation (PI) values were spatially averaged for the urban and rural areas in each region. The trend in the PI changes relative to the WMO base period (1961–1990) mean was estimated for each month over the 54-year time series (Fig. 7).

All regions are characterized by overall greater trends for urban areas than for rural areas, although there are some exceptions depending on the selected region and month. The estimated trends in the urban areas exhibit larger increases than do those in the rural areas during the recent multi-decadal period.

4. Discussion

4.1. Extreme precipitation indices

This study investigates extreme precipitation events in the Netherlands over the past 54 years using extreme precipitation indices. The trends in these indices over the 54-year period are not significant for all the stations throughout the country. However, certain indices show statistically significant changes in local areas where heavy precipitation amounts and intensity have increased over the past 54 years. All of the extreme precipitation indices indicate that conditions became wetter in the Netherlands from 1961 to 2014, especially during the recent years. The changes in indices are probably related to the changes in the atmospheric circulation (such as NAO) and the sea surface temperature (van Haren et al., 2013). In addition, urban land use can lead to greater precipitation (Daniels et al., 2015a,b).

4.2. Index changes in recent decades

The calculated changes in the indices during the two multi-decadal

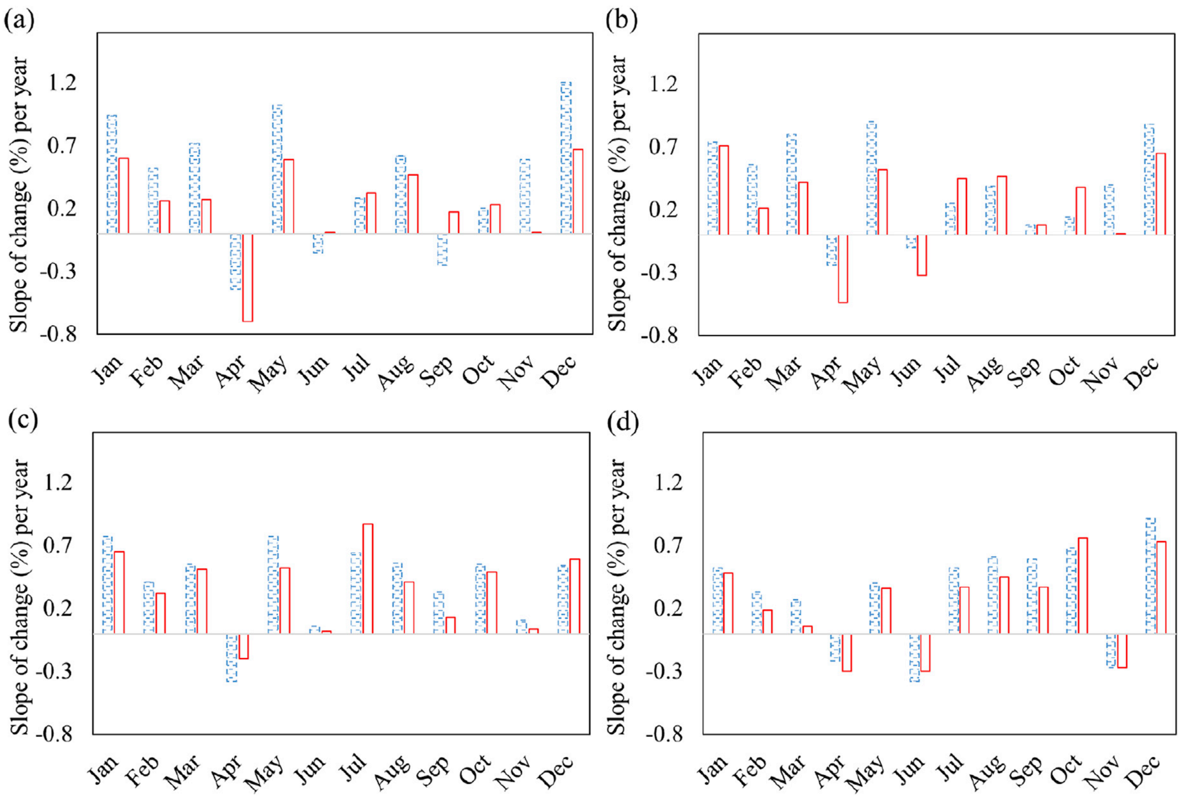

Fig. 7. The slope of PI changes relative to the 1961–1990 average for the urban (blue dashed columns) and rural (red columns) stations in different regions (A, B, C, and D) between 1961 and 2014. The slopes were calculated using the Theil–Sen's slope.

periods (i.e., III and II) can be used to investigate coherent changes in extreme precipitation. The comparison of the two periods shows that the recent multi-decadal period generally has relatively stronger trends and larger values than the earlier period. A prevailing pattern of significant positive changes in the indices is present in the recent multi-decadal period in the Netherlands (Fig. 3).

Among the indices, Px1 was used to analyse the details of the extreme precipitation changes in each month (Fig. 4). The Px1 values revealed that a greater number of extreme precipitation events occurred in period III than in period II. Additionally, extreme precipitation events in the Netherlands occurred most frequently in the summer half-year (especially July and August) during the recent multi-decadal period (period III). The monthly Px1 amounts and trends increased more dramatically over the recent multi-decadal period than over the previous one. Therefore, period II was relatively dry, whereas period III was relatively wet. In other words, the observed discrepancy between the two multi-decadal periods in this study could be driven by the available low frequency of extreme precipitation in Europe from 1970-1980 and the high frequency of extreme precipitation from 1990-2000 (Willems, 2013a,b).

The estimated trend during period III are larger than that in period II in particular for the summer half-year. Similar decadal changes in the Netherlands have been studied by Lenderink et al. (2009). Their results showed that the precipitation trends have been closely related to SSTs since the 1950s. As a natural source of variability, atmospheric circulation could influence the decadal precipitation patterns. Therefore, the greater increase in index trends during period III may be due to variations in atmospheric circulation. The link between cyclonic westerly circulation and precipitation found by Attema and Lenderink (2014) represents a possible physical mechanism for the mentioned periods (August to November). The smaller change in monthly Px1 in the winter half-year during the recent multi-decadal period (III), relative to the previous one (II) may be related to the effects of NAO. The NAO index increased notably before the early 1990s and decreased strongly in recent decades.

4.3. Urban-impacted indices

The well-known causes behind the precipitation changes and possible physical mechanisms (such as circulation, sea and land surface temperatures) were investigated in previous studies (such as Attema et al., 2014; Daniels et al., 2014). In this study, the effects of different land use types on the variability of the indices are quantified based on the differences between the urban and rural areas in the Netherlands according to the CORINE land cover classification. More specifically, Daniels et al. (2014) found that precipitation changes are more greatly affected by the distance from the coast than by other surface characteristics in the Netherlands. To separate this "distance from the coast" effect from the investigation of the impact of urban land use on extreme precipitation, the urban and rural stations were divided into the four regions in terms of their location and distance from the coast. Consequently, the urban and rural areas in each region are affected by approximately similar external influences (such as the NAO (Hurrell, 1995), SSTs (Lenderink et al., 2009), and circulation variability (van Haren et al., 2013)). The changes in the trends of the extreme precipitation indices relative to the 1961–1990 average are larger in the urban areas than in the rural areas over the last 54 years (see section 3.3).

The four defined regions were used to disentangle the coast-inland precipitation gradient from the differences in urban and rural stations. The results demonstrate that the urban influence might have contributed to the observed increase in extreme precipitation. The larger significant changes in most indices and the larger monthly Px1 amounts in the urban areas relative to the rural areas in the same regions can be attributed to the urban impacts on precipitation.

Urban area development occurred in the Netherlands during the recent multi-decadal period (Feranec et al., 2007), and Hazeu and Wit (2004) detected a 4.76% change in the land surface between 1986 and 2000. Additionally, Daniels et al. (2015) found that the urban land use along the west coast of the Netherlands increased from 14% in 1960 to

33% in 2010. This increase in urban land use might have contributed to influences on the local climate. The patterns of index changes in the urban and rural areas differ among the four investigated regions. In the populated western part of the Netherlands, the urban areas were found to have received more intense extreme precipitation than the rural areas. The areas with the largest populations lie along the western coast of the Netherlands (CBS, 2015). This part of the country (region A) exhibits a large discrepancy between the index changes in urban areas and those in rural areas.

This discrepancy between urban and rural areas highlights the influence of urban areas on the extreme precipitation. Previous studies also observed urban influences on the atmosphere and local climate, such as temperature (Brandsma and Wolters, 2012) and precipitation (Daniels et al., 2015a,b, 2016), in the Netherlands. Therefore, in addition to other external factors, the land use type should be treated as an external signal that affects extreme precipitation patterns. Future work using high spatial and temporal resolution data could be performed to determine the urban influences on extreme precipitation and the possible physical mechanisms associated with this process.

5. Conclusions

The extreme precipitation analysis shows that frequency and magnitude of extreme events significantly increased in certain parts of the country, especially in the western urbanised areas of the country. This study shows that the slopes of the index changes relative to the 1961–1990 average in the Netherlands were positive. For both urban and rural areas, the indices follow the same pattern of changes during the two multi-decadal periods. However, the indices in the urban areas have changed to a greater degree than have those in the rural areas during the recent multi-decadal period. The monthly maxima of daily precipitation indicate that the greatest increases occurred in August. The monthly Px1 events increased more during the recent multi-decadal period than during the earlier one for the entire country. In addition, the differences in the monthly Px1 amounts and trends between the two multi-decadal periods are higher in the late summer and autumn.

Overall, larger trends are present in the extreme precipitation indices in urban areas than in those in rural areas. The monthly maxima of daily precipitation were greater in the urban areas than in the rural areas in the Netherlands. This study investigated the impacts of urban land use on Px1 in terms of different regions. The extreme precipitation differences between the urban and rural areas were persistent but varied from region to region. In all the regions, the urban areas received more intense extreme precipitation than did the rural areas, but the observed discrepancy was rarely significant and depended on the region. The Px1 data indicate that a relatively larger discrepancy between urban and rural areas was present in the western densely urbanised region relative to the other regions. The patterns and changes in extreme precipitation, which are strongly dependent on the selected periods and regions, were clearly affected by urban land use in the Netherlands.

Acknowledgements

The authors would like to thank two anonymous reviewers for their constructive comments on an earlier version of this manuscript.

References

Aguilar, E., Aziz Barry, A., Brunet, M., Ekang, L., Fernandes, A., Massoukina, M., Mbah, J., Mhanda, A., do Nascimento, D.J., Peterson, T.C., Thamba Umba, O., Tomou, M., Zhang, X., 2009. Changes in temperature and precipitation extremes in western central Africa, Guinea Conakry, and Zimbabwe, 1955–2006. J. Geophys. Res. 114, D02115. http://dx.doi.org/10.1029/2008JD011010.

Arnbjerg-Nielsen, K., Willems, P., Olsson, J., Beecham, S., Pathirana, A., Bülow Gregersen, I., Madsen, H., Nguyen, V.T.V., 2013. Impacts of climate change on rainfall extremes and urban drainage systems: a review. Water Sci. Technol. 68, 16–28. http://dx.doi.org/10.2166/wst.2013.251.

Attema, J.J., Lenderink, G., 2014. The influence of the North Sea on coastal precipitation in The Netherlands in the present-day and future climate. Clim. Dyn. 42, 505–519. http://dx.doi.org/10.1007/s00382-013-1665-4.

Attema, J.J., Loriaux, J.M., Lenderink, G., 2014. Extreme precipitation response to climate perturbations in an atmospheric mesoscale model. Environ. Res. Lett. 9, 14003. http://dx.doi.org/10.1088/1748-9326/9/1/014003.

Brandsma, T., Wolters, D., 2012. Measurement and statistical modeling of the urban heat island of the city of Utrecht (Netherlands). J. Appl. Meteorol. Climatol. 51, 1046–1060. http://dx.doi.org/10.1175/JAMC-D-11-0206.1.

Buishand, T.A., De Martino, G., Spreeuw, J.N., Brandsma, T., 2013. Homogeneity of precipitation series in The Netherlands and their trends in the past century. Int. J. Climatol. 33, 815–833. http://dx.doi.org/10.1002/joc.3471.

Burauskaite-Harju, A., Grimvall, A., Brömssen, C. Von, 2012. A test for network-wide trends in rainfall extremes. Int. J. Climatol. 32, 86–94. http://dx.doi.org/10.1002/joc.2263.

CBS, 2015. Toelichting Wijk- en en 2015. www.cbs.nl.

Chen, H., Sun, J., Chen, X., Zhou, W., 2012. CGCM projections of heavy rainfall events in China. Int. J. Climatol. 32, 441–450. http://dx.doi.org/10.1002/joc.2278.

Chrysanthou, A., Van Der Schrier, G., Van Den Besselaar, E.J.M., Klein Tank, A.M.G., Brandsma, T., 2014. The effects of urbanization on the rise of the European temperature since 1960. Geophys. Res. Lett. 41, 7716–7722. http://dx.doi.org/10.1002/2014GL061154.

Daniels, E.E., 2016. Land Surface Impacts on Precipitation in the Netherlands.

Daniels, E.E., Lenderink, G., Hutjes, R.W.A., Holtslag, A.A.M., 2014. Spatial precipitation patterns and trends in The Netherlands during 1951-2009. Int. J. Climatol. 34, 1773–1784. http://dx.doi.org/10.1002/joc.3800.

Daniels, E.E., Hutjes, R.W.A., Lenderink, G., Ronda, R.J., Holtslag, A.A.M., 2015a. Land surface feedbacks on spring precipitation in The Netherlands. J. Hydrometeorol. 16, 232–243. http://dx.doi.org/10.1175/JHM-D-14-0072.1.

Daniels, E.E., Lenderink, G., Hutjes, R.W.A., Holtslag, A.A.M., 2015b. Short Communication Observed urban effects on precipitation along the Dutch West coast. Int. J. Climatol. Int. J. Clim. 2119, 2111–2119. http://dx.doi.org/10.1002/joc.4458.

De Lima, M.I.P., Carvalho, S.C.P., De Lima, J.L.M., Coelho, S., 2010. Trends in precipitation: analysis of long annual and monthly time series from mainland Portugal. Adv. Geosci 25, 155–160. http://dx.doi.org/10.5194/adgeo-25-155-2010.

EEA, 2014. CORINE Land Cover Nomenclature Illustrated Guide 1–96.

Feranec, J., Hazeu, G., Christensen, S., Jaffrain, G., 2007. Corine land cover change detection in Europe (case studies of The Netherlands and Slovakia). Land use policy 24, 234–247. http://dx.doi.org/10.1016/j.landusepol.2006.02.002.

R Foundation for Statistical Computing, Vienna, A.I. 3-900051-07-0, 2011. R development core team. R a lang. Environ. Stat. Comput. 55, 275–286.

Griffiths, G.M., Chambers, L.E., Haylock, M.R., Manton, M.J., Nicholls, N., Baek, H.J., Choi, Y., Della-Marta, P.M., Gosai, A., Iga, N., Lata, R., Laurent, V., Maitrepierre, L., Nakamigawa, H., Ouprasitwong, N., Solofa, D., Tahani, L., Thuy, D.T., Tibig, L., Trewin, B., Vediapan, K., Zhai, P., 2005. Change in mean temperature as a predictor of extreme temperature change in the Asia-Pacific region. Int. J. Climatol. 25, 1301–1330. http://dx.doi.org/10.1002/joc.1194.

Groisman, P.Y., Karl, T.R., Easterling, D.R., Knight, R.W., Jamason, P.F., Hennessy, K.J., Suppiah, R., Page, C.M., Wibig, J., Fortuniak, K., Razuvaev, V.N., Douglas, A., Førland, E., Zhai, P.M., 1999. Changes in the probability of heavy precipitation: important indicators of climatic change. Clim. Change. http://dx.doi.org/10.1023/A:1005432803188.

Gutowski, W.J., Arritt, R.W., Kawazoe, S., Flory, D.M., Takle, E.S., Biner, S.S., Caya, D., Jones, R.G., Laprise, R.R., Leung, L.R., Mearns, L.O., Moufouma-Okia, W., Nunes, A.M.B., Qian, Y., Roads, J.O., Sloan, L.C., Snyder, M. a., Raymond, A.L., Ruby, L., Gutowski Jr., W.J., 2010. Regional extreme monthly precipitation simulated by NARCCAP RCMs. J. Hydrometeorol. 11, 1373–1379. http://dx.doi.org/10.1175/2010JHM1297.1.

Hanel, M., Buishand, T.A., 2010. On the value of hourly precipitation extremes in regional climate model simulations. J. Hydrol. 393, 265–273. http://dx.doi.org/10.1016/j.jhydrol.2010.08.024.

Hausfather, Z., Menne, M.J., Williams, C.N., Masters, T., Broberg, R., Jones, D., 2013. Quantifying the effect of urbanization on U.S. Historical Climatology Network temperature records. J. Geophys. Res. Atmos. 118, 481–494. http://dx.doi.org/10.1029/2012JD018509.

Hazeu, G.W., De Wit, A.J.W., 2004. CORINE land cover database of the Netherlands: monitoring land cover changes between 1986 and 2000. EARSeL eProc, 3, 382–387.

Hurk, van den Bart, P.S., Tank, A.K. (Eds.), 2014. KNMI'14 : Climate Change Scenarios for the 21st Century - a Netherlands Perspective 115.

Hurrell, J.W., 1995. Decadal trends in the North atlantic oscillation: regional temperatures and precipitation. Science 269, 676–679. http://dx.doi.org/10.1126/science.269.5224.676.

Jenkinson, A.F., 1955. The frequency distribution of the annual maximum (or minimum) values of meteorological elements. R. Meteorol. Soc. 81, 158–171. http://dx.doi.org/10.1002/qj.49708134804.

Jones, P.D., Jonsson, T., Wheeler, D., 1997. Extension to the North Atlantic oscillation using early instrumental pressure observations from Gibraltar and south-west Iceland. Int. J. Climatol. 17, 1433–1450. http://dx.doi.org/10.1002/(SICI)1097-0088(19971115)17, 13<1433::AID-JOC203>3.0.CO;2-P.

Kendall, M.G., 1948. Rank Correlation Methods. Griffin, Oxford, England.

Klein Tank, A.M.G., Wijngaard, J.B., Konnen, G.P., Bohm, R., Demaree, G., Gocheva, A., Mileta, M., Pashiardis, S., Hejkrlik, L., Kern-Hansen, C., Heino, R., Bessemoulin, P., Muller-Westermeier, G., Tzanakou, M., Szalai, S., Palsdottir, T., Fitzgerald, D., Rubin, S., Capaldo, M., Maugeri, M., Leitass, A., Bukantis, A., Aberfeld, R., van Engelen, A.F.V., Forland, E., Mietus, M., Coelho, F., Mares, C., Razuvaev, V., Nieplova, E., Cegnar, T., Antonio Lopez, J., Dahlstrom, B., Moberg, A., Kirchhofer, W., Ceylan, A., Pachaliuk, O., Alexander, L.V., Petrovic, P., 2002. Daily dataset of 20th-century surface air temperature and precipitation series for the European Climate Assessment. Int. J. Climatol. 22, 1441–1453. http://dx.doi.org/10.1002/joc.773.

Klein Tank, A.M.G., Zwiers, F.W., Zhang, X., 2009. Guidelines on Analysis of Extremes in a Changing Climate in Support of Informed Decisions for Adaptation, Climate Data and Monitoring. World Meteorological Organization.

Lenderink, G., van Meijgaard, E., Selten, F., 2009. Intense coastal rainfall in The Netherlands in response to high sea surface temperatures: analysis of the event of August 2006 from the perspective of a changing climate. Clim. Dyn. 32, 19–33. http://dx.doi.org/10.1007/s00382-008-0366-x.

Levizzani, V., Amorati, R., Meneguzzo, F., 2002. A review of satellite-based rainfall estimation methods. Comm. Proj. Music 70.

Mann, H.B., 1945. Nonparametric tests against trend. Econometrica 13, 245–259. http://dx.doi.org/10.2307/1907187.

Maragatham, R.S., 2012. Trend analysis of rainfall data -a comparative study of existing methods. Int. J. Phys. Math. Sci. 2, 13–18.

Min, S.-K., Zhang, X., Zwiers, F.W., Friederichs, P., Hense, A., 2009. Signal detectability in extreme precipitation changes assessed from twentieth century climate simulations. Clim. Dyn. 32, 95–111. http://dx.doi.org/10.1007/s00382-008-0376-8.

Min, S.-K., Zhang, X., Zwiers, F.W., Hegerl, G.C., 2011. Human contribution to more-intense precipitation extremes. Nature 470, 378–381. http://dx.doi.org/10.1038/nature09763.

Mitra, C., Shepherd, J.M., Jordan, T., 2012. On the relationship between the premonsoonal rainfall climatology and urban land cover dynamics in Kolkata city, India. Int. J. Climatol. 32, 1443–1454. http://dx.doi.org/10.1002/joc.2366.

Nicholls, N., Alexander, L., 2007. Has the climate become more variable or extreme? Progress 1992-2006. Prog. Phys. Geogr. 31, 77–87. http://dx.doi.org/10.1177/0309133307073885.

Oke, T.R., 1982. The energetic basis of the urban heat island. Q. J. R. Meteorol. Soc. 108, 1–24. http://dx.doi.org/10.1002/qj.49710845502.

Rahimpour Golroudbary, V., Zeng, Y., Mannaerts, C.M., Su, Z. (Bob), 2016. Attributing seasonal variation of daily extreme precipitation events across The Netherlands. Weather Clim. Extrem 1–11. http://dx.doi.org/10.1016/j.wace.2016.11.003.

Schneider, A., Friedl, M.A., Potere, D., 2009. A new map of global urban extent from MODIS satellite data. Environ. Res. Lett. 4, 44003. http://dx.doi.org/10.1088/1748-9326/4/4/044003.

Sen, P.K., 1968. Estimates of the regression coefficient based on Kendall's tau. J. Am. Stat. Assoc. 63, 1379–1389. http://dx.doi.org/10.2307/2285891.

Shepherd, J.M., 2006. Evidence of urban-induced precipitation variability in arid climate regimes. J. Arid. Environ. 67, 607–628. http://dx.doi.org/10.1016/j.jaridenv.2006.03.022.

Sluiter, R., 2009. Interpolation methods for climate data: a literature review. KNMI, R&D Information. Obs. Technol. 1–28.

Sluiter, R., 2012. Interpolation Methods for the Climate Atlas. KNMI Tech. Rapp. TR–335, R. Netherlands Meteorol. Institute. Bilt 1–71.

Sluiter, R., 2014. Product Description KNMI14 Daily Grids. KNMI Technical report TR-346.

Suomi, J., Hjort, J., Käyhkö, J., 2012. Effects of scale on modelling the urban heat island in Turku, SW Finland. Clim. Res. 55, 105–118. http://dx.doi.org/10.3354/cr01123.

Ter Maat, H.W., Moors, E.J., Hutjes, R.W. a., Holtslag, a. a. M., Dolman, a. J., 2013. Exploring the impact of land cover and topography on rainfall maxima in The Netherlands. J. Hydrometeorol. 14, 524–542. http://dx.doi.org/10.1175/JHM-D-12-036.1.

Theil, H., 1950. A rank-invariant method of linear and polynomial regression analysis. I. Nederl. Akad. Wetensch., Proc. 53, 386–392. http://dx.doi.org/10.1007/978-94-011-2546-8.

Tian, Y.E., Xu, Y., Booij, M.J., Zhang, Q., Lin, S., 2011. Trends in Precipitation Extremes and Long-term Memory of Runoff Records in Zhejiang, East China 227–232.

Trenberth, K.E., Smith, L., Qian, T., Dai, A., Fasullo, J., 2007. Estimates of the global water budget and its annual cycle using observational and model data. J. Hydrometeorol. 8, 758–769. http://dx.doi.org/10.1175/JHM600.1.

van den Besselaar, E.J.M., Klein Tank, A.M.G., Buishand, T.A., 2012. Trends in European precipitation extremes over 1951-2010. Int. J. Climatol. 2689. http://dx.doi.org/10.1002/joc.3619 n/a-n/a.

van Haren, R., van Oldenborgh, G.J., Lenderink, G., Collins, M., Hazeleger, W., 2013. SST and circulation trend biases cause an underestimation of European precipitation trends. Clim. Dyn. 40, 1–20.

von Storch, H., 1995. Misuses of statistical analysis in climate research. Anal. Clim. Var. http://dx.doi.org/10.1007/978-3-662-03167-4_2. SE - 2 11–26.

Wang, J., Zhang, X., 2008. Downscaling and projection of winter extreme daily precipitation over North America. J. Clim. 21, 923–937. http://dx.doi.org/10.1175/2007JCLI1671.1.

Westra, S., Alexander, L.V., Zwiers, F.W., 2013. Global increasing trends in annual maximum daily precipitation. J. Clim. 26, 3904–3918. http://dx.doi.org/10.1175/JCLI-D-12-00502.1.

Willems, P., 2013a. Multidecadal oscillatory behaviour of rainfall extremes in Europe. Clim. Change 120, 931–944. http://dx.doi.org/10.1007/s10584-013-0837-x.

Willems, P., 2013b. Adjustment of extreme rainfall statistics accounting for multidecadal climate oscillations. J. Hydrol. 490, 126–133. http://dx.doi.org/10.1016/j.jhydrol.2013.03.034.

Yue, S., Pilon, P., Phinney, B., Cavadias, G., 2002. The influence of autocorrelation on the ability to detect trend in hydrological series. Hydrol. Process 16, 1807–1829. http://dx.doi.org/10.1002/hyp.1095.

Yue, S., Pilon, p., Phinney, b, 2003. Canadian streamflow trend detection: impacts of serial and cross-correlation. Hydrol. Sci. J. 48, 51–63. http://dx.doi.org/10.1623/hysj.48.1.51.43478.

Zhang, X., Yang, F., 2004. RClimDex (1.0) user manual. Clim. Res. Branch Environ. Canada 22, 1–23.

Zhang, X., Aguilar, E., Sensoy, S., Melkonyan, H., Tagiyeva, U., Ahmed, N., Kutaladze, N., Rahimzadeh, F., Taghipour, A., Hantosh, T.H., Albert, P., Semawi, M., Karam Ali, M., Said Al-Shabibi, M.H., Al-Oulan, Z., Zatari, T., Al Dean Khelet, I., Hamoud, S., Sagir, R., Demircan, M., Eken, M., Adiguzel, M., Alexander, L., Peterson, T.C., Wallis, T., 2005. Trends in Middle East climate extreme indices from 1950 to 2003. J. Geophys. Res. 110, D22104. http://dx.doi.org/10.1029/2005JD006181.